PERGAMON

International Journal of Heat and Mass Transfer 45 (2002) 655–666

International Journal of HEAT and MASS TRANSFER

www.elsevier.com/locate/ijhmt

Conjugated heat transfer in circular ducts with a power-law laminar convection fluid flow

N. Luna [a], F. Méndez [b,*], C. Treviño [c]

[a] *Instituto Mexicano del Petróleo, México DF, Mexico*

[b] *Facultad de Ingeniería, UNAM, Departamento de Termoenergia, Ciudad Universitaria, 04510 México DF, Mexico*

[c] *Facultad de Ciencias, UNAM, 04510 México DF, Mexico*

Received 17 November 2000; received in revised form 19 March 2001

Abstract

This work deals with the study of the steady-state analysis of conjugated heat transfer process for the thermal entrance region of a developed laminar-forced convection flow of a power-law fluid in a circular tube. A known uniform heat flux is applied at the external surface of the tube. The energy equation in the fluid is solved analytically using the integral boundary layer approximation by neglecting the heat generation by viscous dissipation and the axial heat conduction in the fluid. This solution is coupled to the Laplace equation for the solid, where the axial heat conduction effects are taken into account. The governing equations are reduced to an integro-differential equation which is solved by analytical and numerical methods. The results are shown for different parameters such as conduction parameter, α, the aspect ratio of the tube, ε and the index of power-law fluid, n. © 2001 Published by Elsevier Science Ltd.

1. Introduction

In a broad variety of chemical and industrial processes, non-Newtonian fluids have to be heated or cooled and interesting examples related with the heat transfer characteristics of non-Newtonian fluid flows in pipes appear in double pipe and shell and tube heat exchangers. For instance, in the polymer and food industries it is possible in these geometries to generate well-defined heat transfer rates, which have a strong influence to control extrusion processes. Sometimes, it may also be necessary to reduce the rate at which heat is lost from a pipe system or using another physical configuration, such as screw conveyors. Other typical example where the influence of the heat transfer rates in circular tubes plays an important role occurs in the obstruction of pipelines due to paraffin or wax deposition during the flow of crude oil, recently analyzed by Elphingstone et al. [1] and Ribeiro et al. [2], among others. Many of these applications, including fundamental aspects, are well discussed and documented in a book of Chhabra and Richardson [3], also in detailed surveys by Cho and Hartnett [4], Hartnett and Cho [5], Lawal and Mujumdar [6] and in the Skelland's classical book [7]. Recently, Chhabra [8] presents an excellent review up to date of heat and mass transfer in non-Newtonian flows. However, in all these examples the heat transfer to/from non-Newtonian fluids in circular pipes can be influenced, among others physical aspects, by the finite thermal conductivity of the container. Therefore, the conventional assumptions of no interaction of conduction–convection coupled effects is not realistic and has to be considered in evaluating the conjugate heat transfer processes in the above-mentioned devices. In general, these heat transfer mechanisms have been artificially decoupled in many published works, as the laminar-forced convection heat transfer from circular pipes with prescribed surface temperature or heat flux.

In the past, the solutions of this kind of problems with prescribed boundary conditions, have been classified in fully developed laminar heat transfer and the laminar heat transfer in the thermal entrance region, both with a fully developed velocity profile using the power-law fluid model. This power-law model is

* Corresponding author. Tel: +52-56228103; fax: +52-56228106.

E-mail address: fmendez@servidor.unam.mx (F. Méndez).

0017-9310/02/$ - see front matter © 2001 Published by Elsevier Science Ltd.
PII: S0017-9310(01)00147-8

Nomenclature

c	specific heat of the power-law fluid
dP/dz	axial pressure gradient in the fluid
Gz	Graetz number defined by $Gz = \pi RPe/L$
h	thickness of the tube wall
k	consistency factor introduced in Eq. (1)
L	length of the tube introduced in Eq. (2)
n	power-law index of the non-Newtonian fluid introduced in Eq. (1)
Nu	Nusselt number defined in Eq. (21)
Pe	Peclet number defined by $Pe = \rho c\overline{u}R/\lambda$
q_e	uniform heat flux applied at the external surface of the tube
R	internal radius of the tube
T	temperature
T_∞	entrance temperature of the power-law fluid
T_b	bulk temperature of the power-law fluid
$\overline{u}$	average velocity of the power-law fluid
u	velocity
r, z	cylindrical coordinates

Greek symbols

α	heat conduction or conjugated parameter, defined in Eq. (6)
δ	thickness of the thermal layer in the power-law fluid, defined in Eq. (2)
ε	aspect ratio of the wall, defined in Eq. (6)
ε_0	aspect ratio of the wall, defined in Eq. (6)
λ	thermal conductivity of the power-law fluid
λ_w	thermal conductivity of the tube
ρ	density of the power-law fluid
σ	non-dimensional coordinate, defined in Eq. (12)
θ	non-dimensional temperature of the power-law fluid, defined in Eq. (13)
θ_w	non-dimensional temperature of the wall, defined in Eq. (13)
χ	non-dimensional coordinate, defined in Eq. (12)
ζ	non-dimensional coordinate, defined in Eq. (12)

Subscripts

e	refers to external conditions
f	refers to the fluid
l	conditions at the upward end of the wall
w	conditions at the tube wall

adequate to account the shear dependence of viscosity in most engineering design calculations. Other models using Bingham fluids or more sophisticated rheological cases can also be considered. Here, we analyze only the case of the thermal entrance region with fully developed flow in a tube. Since the experimental work of Pigford [9] to study the thermal entrance flow region with the boundary condition of constant wall temperature, extensive studies of those pre-determined boundary conditions for the involved surfaces have been developed in order to have a better knowledge of these processes.

The first analytical study extending the Newtonian solution to purely viscous power-law fluids was obtained by Bird [10], using a series form solution of the governing equations of the laminar heat transfer in the thermal entrance region for the constant heat flux condition. Bird et al. [11] applied the so-called Leveque-approximation [12] to calculate the laminar heat transfer for the case of constant wall heat flux as well as for constant wall temperature in power-law fluids. The key assumption in this approach is that the thermal boundary layer is confined to a thin layer adjacent to the tube wall. This is a suitable assumption for high flow rates and short tubes, that is for large values of the Graetz number, Gz, to be defined later.

These above laminar heat transfer results in the thermally developing region was reviewed by Bird [13]. Metzner et al. [14] presented the first theoretical analysis combined with an experimental study of the variables controlling heat transfer rates to non-Newtonian fluids. Following the work of Metzner et al. [14], Mahalingam et al. [15] improved the theory using analytical and experimental studies, by comparing with previous relationships and correlations. The chosen wall boundary conditions involved uniformly constant heat flux and step change in surface heat flux. Changing the boundary condition for constant wall temperature, Richardson [16] solved the problem of heat transfer of a power-law fluid in laminar flow, including the effect of heat generation by viscous dissipation. A similar analysis with the same effect for high Prandtl number of the fluid was performed by Basu and Roy [17]. Extended solutions were investigated by Liou and Wang [18], Lawal and Mujumdar [19] and Barletta [20]. On the other hand, the effect of axial heat conduction in the fluid was considered by Johnston [21] and Bilir [22], who showed that this effect is important only very close to the inlet section. Recently, a new analytical solution for the heat transfer in the entrance region for ducts was reported by Khellaf and Lauriat [23], using separation of variables and spectral decomposition of the eigenfunctions in polynomial form.

The study of conjugate heat transfer between forced or natural convection flows and heat conduction in walls is important because of the existence of coupled effects in practical heat transfer processes. In particular, the

design and performance of counterflow multilayered tube heat exchangers offer an excellent opportunity to analyze these phenomena. Using Newtonian flows, the specialized literature have showed many theoretical and experimental analyses to validate the conjugate heat transfer modelling. In this direction and considering simple heat exchanger geometries, Méndez and Treviño [24], Bautista et al. [25] and Treviño et al. [26] have conducted analytical models to elucidate the importance of coupled heat transfer effects. In order to obtain new solutions where non-isothermal conditions at the wall of the tube are present, in this paper we analyze the non-Newtonian conjugate heat transfer between a power-law fluid flowing in a circular tube and the internal wall of the tube. For simplicity, we consider the case for which the external wall of the tube is maintained at an uniform heat flux. We consider here the thermal entrance region with a fully developed laminar velocity profile, neglecting the heat generation by viscous dissipation and the axial heat conduction in the fluid. The axial heat conduction in the tube wall has been considered. We anticipate that the heat flux from the power-law fluid to the wall is strongly influenced by the presence of the wall with finite thermal conductivity, because longitudinal and transverse heat conduction effects become significant. We use perturbation and numerical techniques together with the classical boundary layer theory for the heat transfer analysis of a power-law fluid in a circular tube, to show that the heat transfer is controlled by four non-dimensional parameters: α, n, ε and ε_0. The conjugated parameter α measures the importance of the longitudinal heat conduction through the tube wall, n is the power-law index and ε and ε_0 are aspect ratios very small compared with unity, to be defined later.

2. Formulation and order of magnitude estimates

The physical model under study is shown in Fig. 1. We consider a laminar flow of a power-law fluid along a circular tube with internal radius R and thickness h. The fluid enters to the non-isothermal finite section of length L of the tube with a well-known fully developed velocity profile and stress–strain relationship given by [20]:

$$u = \frac{3n+1}{n+1}\overline{u}\left[1-\left(\frac{r}{R}\right)^{(n+1)/n}\right], \quad \tau_{rz} = k\left|\frac{\mathrm{d}u}{\mathrm{d}r}\right|^{n-1}\frac{\mathrm{d}u}{\mathrm{d}r} \qquad (1)$$

with

$$\overline{u} = \left[\frac{1}{2k}\left(-\frac{\mathrm{d}P}{\mathrm{d}z}\right)\right]^{1/n}\left(\frac{n}{3n+1}\right)R^{(n+1)/n}$$

representing the mean value of the velocity, n is the power-law index ($n = 1$ corresponds to a Newtonian fluid), k is the consistency factor, frequently used in these applications. The origin of the cylindrical coordinates system is placed at the z symmetry axis of the tube and r axis points out in the radial direction, which is normal to the surface of the tube. We assume that prior to the entry plane ($z < 0$), the fluid temperature is uniform, $T_\mathrm{f} = T_\infty$. For $z > 0$, the temperature of the fluid varies in both radial and axial directions as a result of the heat loss q_e from the external wall of the tube, thus building a thin thermal boundary layer at the internal surface of the tube. For simplicity, the fluid properties are assumed to be constant. Both ends of the tube are connected with adiabatic walls, which are the continuation of the non-isothermal wall as shown in Fig. 1.

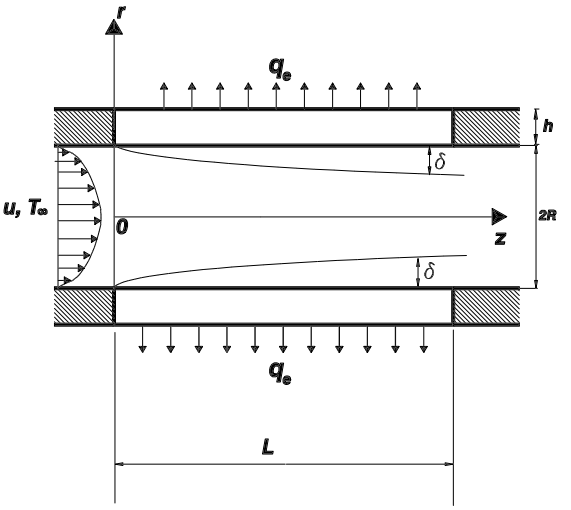

Fig. 1. Schematic diagram of the studied physical model.

In order to obtain the relevant non-dimensional parameters and the working regimes, we introduce an order of magnitude analysis [27]. Using the linearized version of Eq. (1), the characteristic fluid velocity within the thermal boundary layer is given as $u_\mathrm{c} \sim (3n+1)\overline{u}\delta/(nR)$, where δ is the thickness of the thermal boundary layer. Performing an energy balance between the convection and diffusion terms, we obtain that the thermal boundary layer of the fluid is related to the length of the tube as

$$\frac{\delta}{L} \sim \left[\frac{n}{3n+1}\left(\frac{R}{L}\right)^2\frac{1}{Pe}\right]^{1/3}, \qquad (2)$$

where Pe is the well-known Peclet number defined as $Pe = \rho c\overline{u}R/\lambda$. ρ, c and λ represent the density, the specific heat capacity and the thermal conductivity of the fluid, respectively. Due to the adiabatic boundary conditions at both ends of the wall, the overall heat transfer from fluid to the tube wall have to be of the same order of magnitude

$$\lambda\frac{\Delta T_\mathrm{f}}{\delta} \sim \lambda_\mathrm{w}\frac{\Delta T_\mathrm{w}}{h} \sim q_\mathrm{e}, \qquad (3)$$

where ΔT_f and ΔT_w are the characteristic temperatures changes in the transverse direction for the fluid and the wall, respectively. In relationships (3) we assumed that the thermal boundary layer thickness as well as the thickness of the tube are very small compared with the radius of the tube. On the other hand, the total temperature change in the system is then of order $\Delta T \sim \Delta T_f + \Delta T_w$. Combining the relationships (3) with the above total temperature change, ΔT, we can easily show that

$$\frac{\Delta T_w}{\Delta T} \sim 1 \Bigg/ \left[1 + \frac{\alpha}{\varepsilon^2}\left(\frac{n}{3n+1}\right)^{1/3}\right],$$
$$\frac{\Delta T_f}{\Delta T} \sim \left[\frac{\alpha}{\varepsilon^2}\left(\frac{n}{3n+1}\right)^{1/3}\right] \Bigg/ \left[1 + \frac{\alpha}{\varepsilon^2}\left(\frac{n}{3n+1}\right)^{1/3}\right] \tag{4}$$

and the global temperature change must be then of the order

$$\Delta T \sim \frac{q_e h}{\lambda_w}\frac{(1+\varepsilon_0)}{(1+\varepsilon_0/2)}\left[1 + \frac{\alpha}{\varepsilon^2}\left(\frac{n}{3n+1}\right)^{1/3}\right], \tag{5}$$

where α is the longitudinal heat conduction parameter, ε and ε_0 are the aspect ratios of the wall of the tube, defined as

$$\alpha = \frac{\lambda_w}{\lambda}\frac{h}{L}(1+\varepsilon_0/2)\left[\left(\frac{R}{L}\right)^2 \frac{1}{Pe}\right]^{1/3},$$
$$\varepsilon = \frac{h}{L} \quad \text{and} \quad \varepsilon_0 = \frac{h}{R}, \tag{6}$$

where α measures the effect of the longitudinal heat conduction along the tube wall. For values of $\alpha \gg 1$, the longitudinal heat conduction is very strong, thus not permitting the existence of large temperature gradients at the wall. Otherwise, for values of $\alpha \ll 1$, the longitudinal heat conduction is very weak and thus the corresponding term can be neglected in the energy equation for the tube wall. Because n is in general a non-dimensional parameter of order unity, we choose as global characteristic temperature change, ΔT_c, the larger value of the relationship (5), which corresponds for those values of $\alpha/\varepsilon^2 \gg 1$, that is

$$\Delta T_c = \frac{\alpha}{\varepsilon^2}\frac{(1+\varepsilon_0)}{(1+\varepsilon_0/2)}\frac{q_e h}{\lambda_w}. \tag{7}$$

With this definition of the characteristic temperature change, we can normalize the governing equations introduced in the following section. Finally, the order of magnitude of the non-dimensional heat flux or overall Nusselt number using the suitable global Graetz number, $Gz = \pi RPe/L$, is given by the following relationship:

$$Nu \sim \frac{\Delta T_f}{\Delta T_c}\frac{R}{\delta} \sim \left[\left(\frac{3n+1}{n}\right)\frac{Gz}{\pi}\right]^{1/3}. \tag{8}$$

This derived asymptotic formula for the Nusselt number is the well-known given elsewhere, [4,5]. Some physical consequences of relationships (6) and (8) are the following. If we increase the fluid velocity for fixed geometrical values, the Graetz and Nusselt numbers also increase and the value of α decreases, indicating that the longitudinal heat transfer produces contrary effects on the Nusselt number. We can also obtain interesting asymptotic relevant limits, which dictate the different physical regimes of the conjugated heat transfer process. Basically, we select two different cases: $\alpha/\varepsilon^2 \gg 1$, $\alpha/\varepsilon^2 \sim 1$, with the index n of order unity. For values of $\alpha/\varepsilon^2 \gg 1$, from the relationships (5) and (8) we obtain

$$\frac{\Delta T_w}{\Delta T} \sim \frac{\varepsilon^2}{\alpha}\left(\frac{3n+1}{n}\right)^{1/3} \ll 1, \quad \frac{\Delta T_f}{\Delta T} \sim 1. \tag{9}$$

Thus, the transverse temperature variations in the wall of the tube compared with the overall temperature drop ΔT are very small, of order ε^2/α at most. This represents the so-called thermally thin wall limit [24], where the temperature in the tube wall can be assumed to be only a function of the longitudinal coordinate, $T_w(z)$. For values of $\alpha/\varepsilon^2 \sim 1$, we obtain from the same order relationships

$$\frac{\Delta T_w}{\Delta T} \sim 1 \Bigg/ \left[1 + \left(\frac{n}{3n+1}\right)^{1/3}\right] \sim 1,$$
$$\frac{\Delta T_f}{\Delta T} \sim 1 \Bigg/ \left[1 + \left(\frac{3n+1}{n}\right)^{1/3}\right] \sim 1. \tag{10}$$

In the latter case, the transverse temperature drop in the tube is of the order of magnitude than the overall temperature drop for finite values of n. This corresponds to the thermally thick wall limit. The numerical and analytical solutions presented in the following sections validate these asymptotic relationships. In these sections, we solve fully the thermally thin wall regime, using asymptotic and numerical methods. Applying a regular perturbation scheme, the thermally thick wall regime is analyzed only for the case of $\alpha/\varepsilon^2 \ll 1$, i.e., when the local influence of inner zones of longitudinal heat conduction close to both ends of the tube wall, is neglected.

2.1. Governing equations

The non-dimensional governing equations for the wall of the tube and for the non-Newtonian fluid flow, together with the corresponding boundary conditions, are given below. Guided by the order of magnitude estimates, we introduce the following non-dimensional variables:

$$\chi = \frac{z}{L}, \quad \sigma = \frac{r-R}{h},$$
$$\zeta = (R-r) \Bigg/ \left[R \left[\frac{n}{3n+1} \frac{\pi}{Gz} \right]^{1/3} \chi^{1/3} \right], \tag{11}$$

$$\theta = \frac{T_\infty - T}{\Delta T_c}, \quad \theta_w = \frac{T_\infty - T_w}{\Delta T_c}. \tag{12}$$

The resulting non-dimensional energy governing equations for the fluid and the wall are, respectively

$$\frac{\partial^2 \theta}{\partial \zeta^2} + \frac{1}{3}\zeta^2 \frac{\partial \theta}{\partial \zeta} = \chi \zeta \frac{\partial \theta}{\partial \chi}, \tag{13}$$

$$\alpha \frac{\partial^2 \theta_w}{\partial \chi^2} + \frac{\alpha}{\varepsilon^2} \frac{1}{(1+\varepsilon_0 \sigma)} \frac{\partial}{\partial \sigma} \left[(1+\varepsilon_0 \sigma) \frac{\partial \theta_w}{\partial \sigma} \right] = 0. \tag{14}$$

The energy equation for the fluid was derived using the boundary layer approximation for large values of the Graetz number, $Gz \gg 1$, which corresponds to neglect the longitudinal heat conduction along the fluid. This analysis is also called Leveque's approximation in the specialized literature and the thermal boundary layer is confined to a thin layer of the fluid adjacent to tube wall, where the velocity profile can be linearized close to the wall [12,28]. The adiabatic boundary conditions for the wall of the tube are given by $\partial \theta_w / \partial \chi|_{\chi=0,1} = 0$, whereas the boundary conditions associated with the fluid are

$$\theta(0, \zeta) = 0, \quad \theta(\chi, \infty) \to 0, \tag{15}$$

together with

$$\left. \frac{\partial \theta_w}{\partial \sigma} \right|_{\sigma=1} = \frac{\varepsilon^2}{\alpha} \frac{(1+\varepsilon_0/2)}{(1+\varepsilon_0)}. \tag{16}$$

Furthermore, we also need the compatibility conditions at the internal surface of the wall given by the continuity of temperature and heat flux, which can be written as

$$\theta(\chi, 0) = \theta_w(\chi, 0),$$
$$\left. \frac{\partial \theta_w}{\partial \sigma} \right|_{\sigma=0} = -\frac{\varepsilon^2}{\alpha} \frac{(1+\varepsilon_0/2)}{\chi^{1/3}} \left(\frac{3n+1}{4n} \right)^{1/3} \left. \frac{\partial \theta}{\partial \zeta} \right|_{\zeta=0}. \tag{17}$$

The energy equation for the fluid (13) can be easily integrated by using the Lighthill's integral technique [28]. For this specific case, the non-dimensional heat flux at the inner surface of the wall can be written as

$$\left. \frac{\partial \theta}{\partial \zeta} \right|_{\zeta=0} = -0.8546 \left[\theta_{wl} + \int_0^\chi K(\chi, \chi') \frac{d\theta'_w(\chi', 0)}{d\chi'} d\chi' \right], \tag{18}$$

where the kernel K is a function given by $K(\chi, \chi') = (1 - \chi'/\chi)^{-1/3}$ and θ_{wl} is the value of the non-dimensional temperature at $\chi = \sigma = 0$. The solution of the problem (13)–(17) should provide

$$\theta_w = F(\chi, \sigma : \alpha, n, \varepsilon, \varepsilon_0) \quad \text{for } Gz \gg 1. \tag{19}$$

The local reduced non-dimensional heat flux or local Nusselt number at the external surface of the wall, is defined as

$$Nu_\chi = \frac{2 q_e R}{\lambda (T_b - T_w(z, R+h))} = \frac{2}{\theta_w(\chi, 1)} \left(\frac{Gz}{\pi} \right)^{1/3}. \tag{20}$$

Therefore, an averaged Nusselt number can also be obtained as

$$Nu = 2 \left(\frac{Gz}{\pi} \right)^{1/3} \int_0^1 \frac{d\chi}{\theta_w(\chi, 1)}, \tag{21}$$

where T_b is the bulk temperature of the stream flow and is close to T_∞ as a first approximation, due to the presence of the thin thermal boundary layer flow. The higher corrections to $T_b - T_\infty$ are of order of $T_\infty Gz^{-1}$, for $Gz \gg 1$, which are not considered in this work.

3. Thermally thin wall limit ($\alpha/\varepsilon^2 \gg 1$)

For values of α very large compared with ε^2, the non-dimensional temperature of the wall depends only on the χ coordinate in a first approximation, as predicted in relationship (9). Therefore, Eq. (14) can be integrated along the transverse coordinate and after applying the boundary and compatibility conditions (16) and (17), together with Eq. (18), we obtain

$$\alpha \frac{d^2 \theta_w}{d\chi^2} + 1 = \frac{C_0}{\chi^{1/3}} \left(\frac{3n+1}{4n} \right)^{1/3} \left[\theta_{wl} + \int_{\theta_{wl}}^{\theta_w} K(\chi, \chi') d\theta'_w \right], \tag{22}$$

where the constant $C_0 = 12^{1/3}/\Gamma(1/3) \doteq 0.8546$ and $\Gamma(a)$ represents the complete Γ-function. The first and second terms at the left-hand side of Eq. (22), denote the longitudinal heat conduction along the wall and the non-dimensional heat removed from the external surface of the tube. Parameter α measures then the influence of the longitudinal heat conduction. The term on the right-hand side is the heat transferred from the fluid. This equation has to be solved together with the adiabatic boundary conditions. Eq. (22) defines one integro-differential equation for the unknown θ_w with two non-dimensional parameters, α and n. In this regime, the aspect ratios ε and ε_0 play no role in the heat transfer process, thus the functional relationship (19) reduces to $\theta_w = F(\chi : \alpha, n)$. For very large values of α, a uniform temperature distribution in the tube wall is obtained, depending only on the index n. In the following sections, we analyze the limits characterized by large and small values of α, with values of n of order unity and $\alpha/\varepsilon^2 \gg 1$. Employing numerical techniques reported elsewhere [29], we solve Eq. (22) and compare with analytical solutions of this equation using asymptotic techniques.

3.1. Solution for $\alpha \gg 1$

For large values of α compared with unity, the non-dimensional temperature of the plate is practically uniform giving only small changes (of the order α^{-1}) in the longitudinal direction, as was anticipated from the order of magnitude analysis. Therefore, θ_w can be obtained by using the following regular expansion series

$$\theta_w(\chi : n) = \theta_0(n) + \sum_{j=1}^{\infty} \alpha^{-j}\theta_j(\chi : n). \tag{23}$$

Introducing these relationships into Eq. (22), we obtain the following set of equations, after collecting terms with the same power of α

$$\frac{d^2\theta_0}{d\chi^2} = 0, \tag{24}$$

$$\frac{d^2\theta_1}{d\chi^2} + 1 = C_0\left(\frac{3n+1}{4n}\right)^{1/3}\chi^{-1/3}\left[\theta_{0l} + \int_{\theta_{1l}}^{\theta_1} K(\chi,\chi')d\theta_0'\right], \tag{25}$$

$$\frac{d^2\theta_{j+1}}{d\chi^2} = C_0\left(\frac{3n+1}{4n}\right)^{1/3}\chi^{-1/3}\left[\theta_{jl} + \int_{\theta_{1l}}^{\theta_1} K(\chi,\chi')d\theta_{j,}'\right] \quad \text{for } j > 0 \tag{26}$$

with the adiabatic boundary conditions

$$\left.\frac{d\theta_j}{d\chi}\right|_{\chi=0,1} = 0 \quad \text{for all } j. \tag{27}$$

Integrating Eq. (24) with the adiabatic boundary conditions (27), gives $\theta_0 = \theta_0(n)$, where the value is to be obtained with the aid of the first-order solution. Integrating Eq. (25) and applying the adiabatic boundaries at both ends of the tube, we obtain the leading order of the non-dimensional tube wall temperature as a function of the power index n in the form

$$\theta_0 = (2/3)^{1/3}\Gamma(4/3)\left(\frac{4n}{3n+1}\right)^{1/3}. \tag{28}$$

Introducing the solution for θ_0 into Eq. (25), and integrating this equation twice, we obtain

$$\theta_1(\chi) = -\frac{1}{2}\chi^2 + \frac{3}{5}\chi^{5/3} + C_1, \tag{29}$$

where C_1 is an integration constant related to the temperature of the tube at $\chi = 0$ and must be determined by solving the second-order equation. Following the same procedure, the value of C_1 is obtained as

$$C_1 = \frac{1}{4}B(2,2/3) - \frac{2}{7}B(5/3,2/3) \doteq -0.0683. \tag{30}$$

Here, $B(a,b)$ represents the complete β-function. The solution for the first-order correction does not depend on the index n. In the same form, $\theta_2(\chi : n)$ is given by

$$\theta_2(\chi : n) = C_0\left(\frac{3n+1}{4n}\right)^{1/3}\left[-\frac{9}{88}\chi^{11/3}B(2,2/3) + \frac{9}{70}\chi^{10/3}B(5/3,2/3) + \frac{9}{10}\chi^{5/3}C_1 + C_2\right], \tag{31}$$

where

$$C_2 = \frac{3}{52}B(2,2/3)B(11/3,2/3) - \frac{1}{14}B(5/3,2/3)B(10/3,2/3) - \frac{3}{7}C_1B(5/3,2/3) \doteq 0.01455. \tag{32}$$

Therefore, up to terms of order α^{-2}, the non-dimensional wall temperature is written as

$$\theta_w(\chi : n) = (2/3)^{1/3}\Gamma(4/3)\left(\frac{4n}{3n+1}\right)^{1/3} + \frac{1}{\alpha}\left(-\frac{1}{2}\chi^2 + \frac{3}{5}\chi^{5/3} + C_1\right) + \frac{C_0}{\alpha^2}\left(\frac{3n+1}{4n}\right)^{1/3} \times \left[-\frac{9}{88}\chi^{11/3}B(2,2/3) + \frac{9}{70}\chi^{10/3}B(5/3,2/3) + \frac{9}{10}\chi^{5/3}C_1 + C_2\right] + O(\alpha^{-3}), \tag{33}$$

whereas the non-dimensional local and averaged heat fluxes up to terms of order α^{-1}, take the form

$$\frac{Nu_\chi}{Gz^{1/3}} = \frac{1.496}{\chi^{1/3}}\left(\frac{3n+1}{4n}\right)^{2/3}\left\{0.78\left(\frac{4n}{3n+1}\right)^{1/3} + \frac{1}{\alpha}\left[-0.4\chi^2 + 0.36\chi^{5/3}\right]\right\} + O(\alpha^{-2}) \tag{34}$$

$$\frac{Nu}{Gz^{1/3}} = \left(\frac{3n+1}{4n}\right)^{1/3}\left[1.7503. + \frac{0.0064}{\alpha}\left(\frac{3n+1}{4n}\right)^{1/3}\right] + O(\alpha^{-2}). \tag{35}$$

The leading term on the right-hand side of the above equations represents the classical Metzner solution for an isothermal tube surface [14]. Eq. (35) shows that the global Nusselt number increases for decreasing values of α.

3.2. Solution for $\alpha \to 0$

For small values of α compared with unity, the longitudinal heat conduction term in Eq. (22) can be neglected in a first approximation. For values of $\alpha \to 0$, but large compared with ε^2, the thermally thin wall

approximation is still valid. This case represents a singular limit due to the existence of two longitudinal heat conducting layers at both ends in order to satisfy the adiabatic boundary conditions. The mathematical model of these thermal boundary layers is not presented here, because they only have a local thermal influence close to the ends. Outside of these regions, longitudinal heat conduction along the wall is always negligible, reducing Eq. (22) to an integral equation

$$\frac{C_0}{\chi^{1/3}}\left(\frac{3n+1}{4n}\right)^{1/3}\left[\int_0^{\theta_{we}} K(\chi,\chi')\mathrm{d}\theta'_{we}\right]=1. \tag{36}$$

The subscript e is used to denote the outer solution, where the longitudinal heat conduction has been removed. We also have to remove the boundary conditions $\mathrm{d}\theta_{we}/\mathrm{d}\chi=0$ at both edges. The above integral equation can be solved by applying the Abel's inversion theorem [30], giving

$$\theta_{we}(\chi:n)=\frac{3\sqrt{3}}{2\pi C_0}\left(\frac{4n}{3n+1}\right)^{1/3}\chi^{1/3}. \tag{37}$$

The local and averaged Nusselt numbers for this regime are then given by:

$$\frac{Nu_\chi}{Gz^{1/3}}=\frac{1.411}{\chi^{1/3}}\left(\frac{3n+1}{4n}\right)^{1/3} \tag{38}$$

$$\frac{Nu}{Gz^{1/3}}=2.1165\left(\frac{3n+1}{4n}\right)^{1/3}. \tag{39}$$

Comparing both averaged Nusselt numbers for large and small values of α, we conclude that the effect of longitudinal heat conduction along the tube walls is to reduce in 17.062% the heat transfer rate.

4. Thermally thick wall limit ($\alpha/\varepsilon^2 \ll 1$)

In this regime, the transverse temperature variations in the wall are of order of the global temperature change, ΔT, and the wall temperature is now a function of the longitudinal and transverse coordinates χ and σ, respectively. However, for small values of ε^2, the longitudinal heat conduction along the tube wall is also very small and can be neglected in the whole length of the wall. The problem is then reduced to analyze the outer non-longitudinal heat conduction region. A first integration of Eq. (22) gives

$$(1+\varepsilon_0\sigma)\frac{\partial\theta_w(\chi,\sigma)}{\partial\sigma}=(1+\varepsilon_0)\left.\frac{\partial\theta_w}{\partial\sigma}\right|_{\sigma=1}=\left.\frac{\partial\theta_w}{\partial\sigma}\right|_{\sigma=0}. \tag{40}$$

Replacing the boundary conditions (16) and (17), together with (18), we obtain an unique integral equation for $\theta_w(\chi,0)$ as

$$\frac{C_0}{\chi^{1/3}}\left(\frac{3n+1}{4n}\right)^{1/3}\left[\int_0^{\theta_w} K(\chi,\chi')\mathrm{d}\theta'_w(\chi',0)\right]=1. \tag{41}$$

This equation is exactly the same as for the thermally thin regime with $\alpha=0$, given by Eq. (37). Integrating the first equality in Eq. (40) and taken into account the known function $\theta_w(\chi,0)$, we get the final solution for the thermally thick regime as

$$\theta_w(\chi,\sigma:n)=\frac{3\sqrt{3}}{2\pi C_0}\left(\frac{4n}{3n+1}\right)^{1/3}\chi^{1/3}+\frac{\varepsilon^2}{\alpha}\frac{(1+\varepsilon_0/2)}{\varepsilon_0}\ln(1+\varepsilon_0\sigma) \tag{42}$$

with the corresponding local Nusselt number given by

$$\frac{Nu_\chi}{Gz^{1/3}}=1\Big/\left[\frac{3\sqrt{3}}{2\pi C_0}\left(\frac{4n}{3n+1}\right)^{1/3}\chi^{1/3}+\frac{\varepsilon^2}{\alpha}\right], \tag{43}$$

where we have omitted the curvature effect represented by ε_0. The resulting averaged Nusselt number is then given by

$$\frac{Nu}{Gz^{1/3}}=\frac{2b}{\pi^{1/3}}\left(\frac{3}{2}-\frac{3\varepsilon^2}{\alpha}b+\frac{3\varepsilon^4}{\alpha^2}b^2\ln\left(\frac{b+\alpha/\varepsilon^2}{b}\right)\right), \tag{44}$$

where

$$b=\frac{2\pi C_0}{3\sqrt{3}}\left(\frac{3n+1}{4n}\right)^{1/3}=1.0334\left(\frac{3n+1}{4n}\right)^{1/3}. \tag{45}$$

For large values of ε^2/α compared with unity, the asymptotic behavior is given by

$$\frac{Nu}{Gz^{1/3}}\sim 1.3656\frac{\alpha}{\varepsilon^2}-0.99109\left(\frac{4n}{3n+1}\right)^{1/3}\left(\frac{\alpha}{\varepsilon^2}\right)^2+\mathrm{O}\left(\frac{\alpha}{\varepsilon^2}\right)^3. \tag{46}$$

The first term corresponds to the case of pure transverse heat conduction. On the other hand for small values of ε^2/α compared with unity, the asymptotic behavior is given by

$$\frac{Nu}{Gz^{1/3}}\sim 2.1167\left(\frac{3n+1}{4n}\right)^{1/3}-4.3748\left(\frac{3n+1}{4n}\right)^{2/3}\frac{\varepsilon^2}{\alpha}+\mathrm{O}\left(\frac{\varepsilon^2}{\alpha}\right)^2 \tag{47}$$

for values of $\alpha/\varepsilon^2 \gg 1$. The first term here corresponds to the limit of thermally thin wall regime with $\alpha=0$.

5. Results and conclusions

The heat transfer process is governed by three non-dimensional parameters: α, ε and n, for values of the Graetz number very large compared with unity.

Parameter α measures the effect of the longitudinal heat conduction along the tube wall as represented by Eq. (22). Therefore, the longitudinal heat conduction is important for not very small values of α compared with unity. The other relevant parameter is given by α/ε^2, which determines the thermal regime in the tube wall. The inverse of this parameter is often called the Brun number or the conjugate parameter. For large values of α/ε^2 compared with unity, the temperature variations in the transverse direction in the tube wall are negligible compared with the global temperature change dictated by the external heat flux. This is what we call the thermally thin wall regime. In this regime, the temperature gradients in the wall are of order $\Delta T_c/\alpha L$, for not very small values of α and of order $\Delta T_c/L$ for small values of α. The largest temperature gradients arise in the thermally thick wall regime with gradients of the order $\Delta T_c/h$. In the limit of very large values of $\alpha \to \infty$, the wall temperature is practically uniform and given in a first approximation by the leading term (28). From this relationship, θ_0, is an increasing function of the power index n, reaching the asymptotic limit of $\theta_0 \sim 0.8586$ for $n \gg 1$. For $n < 1$, i.e. for a shear thinning or pseudoplastic fluid, the wall temperature in physical units is larger than the case of $n > 1$ (shear-thickening or dilatant fluid), indicating a large heating of the wall material for the pseudoplastic case. On the other hand, for values of $\alpha \to 0$, Eq. (22) is singular. This means that it is necessary to include the inner heat conducting layers at both ends of the wall tube. However, these thermal conduction boundary layers have only a local influence and we do not present the solution in these layers. Outside these inner regions, there is an outer zone where the non-dimensional temperature of the wall tube is shown in Fig. 2 as a function of the longitudinal coordinate χ for $\alpha = 0$ and different values of the parameter n. Here, we have used the analytical solution given by Eq. (37). In Fig. 3, we show the numerical and asymptotic solutions of the governing equation (22) for the non-dimensional temperature as a function of the longitudinal coordinate χ for $\alpha = 1$ and different values of the power index n. We also obtain here a similar behavior for the non-dimensional temperature. However, the asymptotic solution for large values of α, gives excellent results confirming that even for values of $\alpha \sim 1$, this solution offers an excellent agreement with the numerical solution. In Fig. 4, the same parametric dependence of the non-dimensional wall temperature is shown for a value of $\alpha = 10$. Obviously, in this case the agreement between both solutions has been improved. For larger values of the parameter α, the non-dimensional temperature tends to reach a uniform value, depending only on the assumed values of the parameter n.

Figs. 5 and 6 show the ratio of $Nu_\chi/Gz^{1/3}$, given by Eq. (38), as a function of the coordinate χ for different values of the parameter n with $\alpha = 0$ and $\alpha = 10$, respectively. For this set of values of the involved non-dimensional parameters α and n, the ratio $Nu_\chi/Gz^{1/3}$ shows a very sensible dependence for very small values

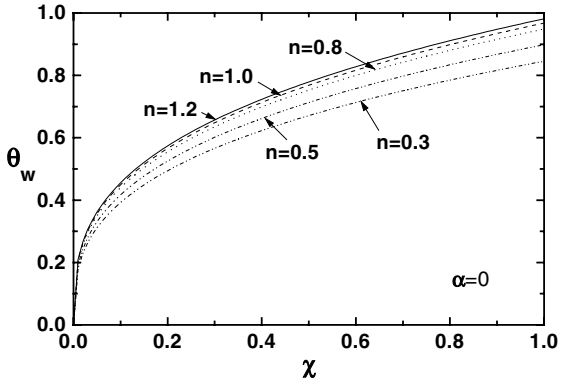

Fig. 2. Non-dimensional wall temperature profile given by Eq. (37) as a function of χ, for $\alpha = 0$ and different values of n.

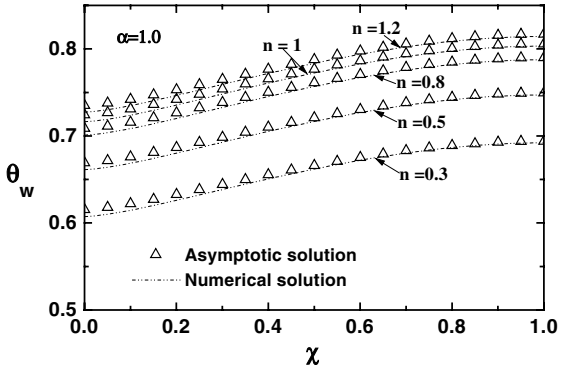

Fig. 3. Numerical and asymptotic non-dimensional wall temperature profiles as a function of the non-dimensional longitudinal coordinate χ, for $\alpha = 1$ and different values of n.

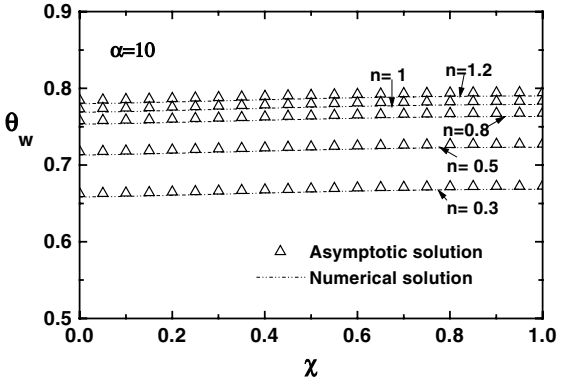

Fig. 4. Numerical and asymptotic non-dimensional wall temperature profiles as a function of the non-dimensional longitudinal coordinate χ, for $\alpha = 10$ and different values of n.

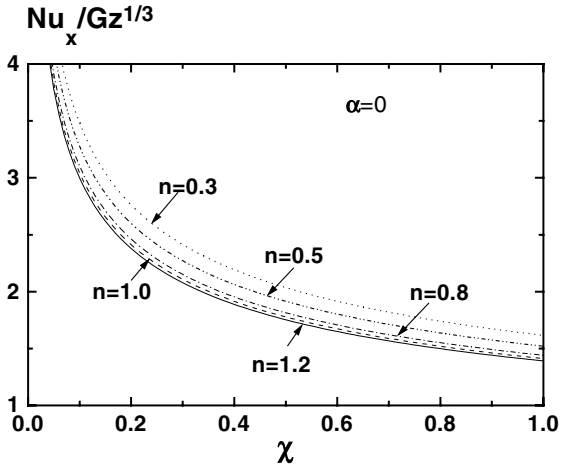

Fig. 5. Local reduced Nusselt number given by Eq. (38) as a function of the non-dimensional longitudinal coordinate χ, for $\alpha = 0$ and different values of n.

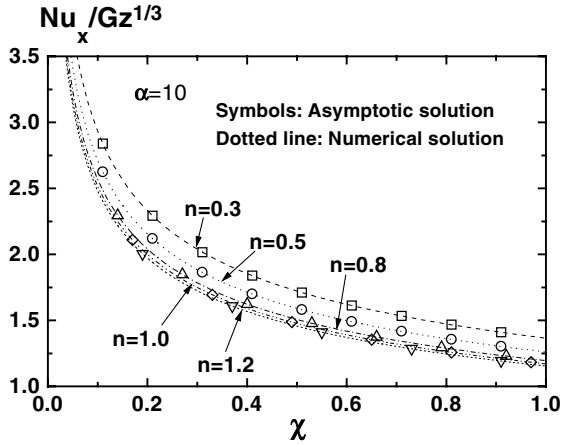

Fig. 6. Numerical and asymptotic local reduced Nusselt number as a function of the non-dimensional longitudinal coordinate χ, for $\alpha = 10$ and different values of n.

of n. In both figures, the numerical and asymptotic solutions compare very well. Fig. 7 shows the global or average ratio $Nu/Gz^{1/3}$ as a function of α for the thermally thin wall regime, for different values of n. Here, we present the numerical and the asymptotic solutions up to terms of order α^{-1} and α^{-2}. In this figure, there are critical values of $\alpha \sim 1$ where the perturbation solutions obtained for large values of α are no longer valid. However, we separate both asymptotic solutions to show that the first-order effects give a better agreement with the numerical solution. We also report in the same figure that obtained asymptotic values for $Nu/Gz^{1/3}$ with $\alpha = 0$, using the formula (38). Clearly, the numerical solution tends to validate the asymptotic relationships.

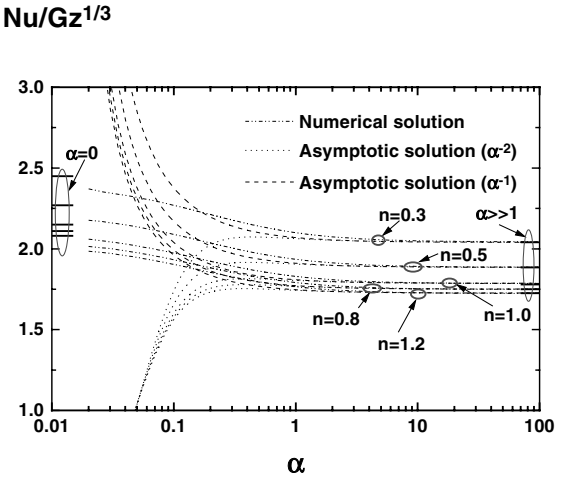

Fig. 7. Numerical and asymptotic values of the global reduced Nusselt number as a function of α and different values of n for the thermall thin wall regime.

Finally in Fig. 8 we show the reduced global Nusselt number $Nu/Gz^{1/3}$ for both the thermally thin and thick wall regimes as a function of α and α/ε^2, respectively. In this case we show the plot for the specific case of $n = 1$. All other values of n produce similar results. For values of α very small compared with ε^2 (thermally thick wall) the global reduced Nusselt number is very low and basically the heat transfer process is due to heat conduction through the tube wall. As the value of α increases, the reduced Nusselt number increases drastically to reach a maximum for values of $1 \gg \alpha \gg \varepsilon^2$. At this point, the longitudinal heat conduction through the wall is negligible because the value of α is still very small compared with unity. As the value of α increases further, the longitudinal heat conduction along the tube wall is

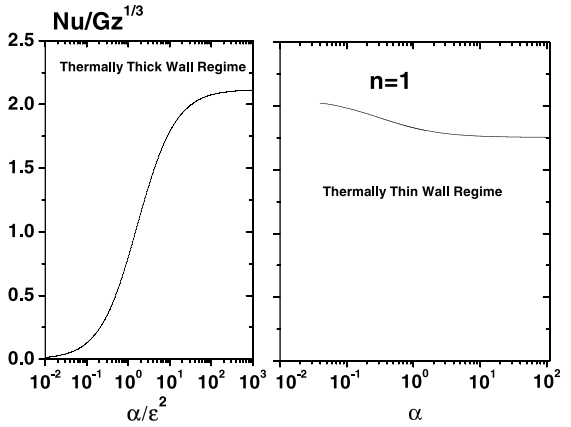

Fig. 8. Global reduced Nusselt number as a function of α and ε for the specific case of $n = 1$. The thermally thin and thick wall regimes are clearly shown.

Table 1
Reduced values of the parameter $Nu/Gz^{1/3}$ compared with the corresponding data reported in [4] for extremely long and short tubes

	Re	*Pr*	*Gz*	α	α/ε^2	*n*	$Nu/Gz^{(1/3)}$ [10]	$Nu/Gz^{(1/3)}$ Eq. (35)	% Error
Reported data [4]: $L/R = 950, h/L = 0.0001$									
Al-Separan	3060.0000	29.2000	2.9548E+02	7.2753E−06	7.2753E+02	0.7870	2.1566	2.1632	0.3071
	986.0000	34.0000	1.1086E+02	1.0087E−05	1.0087E+03	0.7870	2.1566	2.1632	0.3071
	447.0000	37.8000	5.5876E+01	1.2675E−05	1.2675E+03	0.7870	2.1566	2.1632	0.3071
	212.0000	42.2000	2.9585E+01	1.5668E−05	1.5668E+03	0.7870	2.1566	2.1632	0.3071
Cu-Separan	3060.0000	29.2000	2.9548E+02	1.2310E−05	1.2310E+03	0.7870	2.1566	2.1632	0.3071
	986.0000	34.0000	1.1086E+02	1.7067E−05	1.7067E+03	0.7870	2.1566	2.1632	0.3071
	447.0000	37.8000	5.5876E+01	2.1446E−05	2.1446E+03	0.7870	2.1566	2.1632	0.3071
	212.0000	42.2000	2.9585E+01	2.6509E−05	2.6509E+03	0.7870	2.1566	2.1632	0.3071
Al-Polyox	147.0000	29.2000	1.4195E+01	2.0013E−05	2.0013E+03	0.7640	2.1630	2.1696	0.3071
	552.0000	34.0000	6.2065E+01	1.2239E−05	1.2239E+03	0.7640	2.1630	2.1696	0.3071
	1030.0000	37.8000	1.2875E+02	9.5964E−06	9.5964E+02	0.7640	2.1630	2.1696	0.3071
	1830.0000	42.2000	2.5538E+02	7.6377E−06	7.6377E+02	0.7640	2.1630	2.1696	0.3071
Cu-Polyox	147.0000	29.2000	1.4195E+01	3.3862E−05	3.3862E+02	0.7640	2.1630	2.1696	0.3071
	552.0000	34.0000	6.2065E+01	2.0708E−05	2.0708E+03	0.7640	2.1630	2.1696	0.3071
	1030.0000	37.8000	1.2875E+02	1.6237E−05	1.6237E+03	0.7640	2.1630	2.1696	0.3071
	1830.0000	42.2000	2.5538E+02	1.2923E−05	1.2923E+03	0.7640	2.1630	2.1696	0.3071
Short tubes: $R/L = 1, h/L = 0.1$									
Al-Separan	3060.0000	29.2000	2.8071E+05	0.6679	6.6792E+07	0.7870	2.1566	1.7989	16.5833
	986.0000	34.0000	1.0532E+05	0.9261	9.2606E+07	0.7870	2.1566	1.7961	16.7126
	447.0000	37.8000	5.3082E+04	1.1637	1.1637E+08	0.7870	2.1566	1.7947	16.7810
	212.0000	42.2000	2.8106E+04	1.4384	1.4384E+08	0.7870	2.1566	1.7936	16.8319
Cu-Separan	3060.0000	29.2000	2.8071E+05	1.1301	1.1301E+08	0.7870	2.1566	1.7948	16.7731
	986.0000	34.0000	1.0532E+05	1.5669	1.5669E+08	0.7870	2.1566	1.7932	16.8495
	447.0000	37.8000	5.3082E+04	1.9689	1.9689E+08	0.7870	2.1566	1.7923	16.8899
	212.0000	42.2000	2.8106E+04	2.4337	2.4337E+08	0.7870	2.1566	1.7917	16.9200
Al-Polyox	147.0000	29.2000	1.3485E+04	1.8373	1.8373E+08	0.7640	2.1630	1.7979	16.8782
	552.0000	34.0000	5.8962E+04	1.1236	1.1236E+08	0.7640	2.1630	1.8002	16.7707
	1030.0000	37.8000	1.2232E+05	0.8810	8.8101E+07	0.7640	2.1630	1.8019	16.6945
	1830.0000	42.2000	2.4261E+05	0.7012	7.0119E+07	0.7640	2.1630	1.8038	16.6040
Cu-Polyox	147.0000	29.2000	1.3485E+04	3.1088	3.1088E+08	0.7640	2.1630	1.7964	16.9474
	552.0000	34.0000	5.8962E+04	1.9011	1.9011E+08	0.7640	2.1630	1.7978	16.8838
	1030.0000	37.8000	1.2232E+05	1.4907	1.4907E+08	0.7640	2.1630	1.7988	16.8388
	1830.0000	42.2000	2.4261E+05	1.1864	1.1864E+08	0.7640	2.1630	1.7999	16.7853

now important and its effect is to reduce the global reduced Nusselt number reaching a finite value as the value of $\alpha \to \infty$.

By way of illustration we show in Table 1 the influence of the longitudinal heat conduction in the overall process represented by the ratio of $Nu/Gz^{1/3}$. In the upper part of this table, we use the reported data by Cho and Hartnett [4] for extremely long tubes. We computed the respective values of α and α/ε^2 assuming a relative thickness of the tube $h/L = 10^{-4}$ and two different metallic tubes (aluminium and copper). In all experimental cases, the values of α are very low compared with unity but with values of α/ε^2 very large compared with unity. Therefore the solution for $Nu/Gz^{1/3}$ given by Eq. (39), corresponding to the thermally thin wall regime with $\alpha \to 0$ [10], gives an excellent approximation. In the lower part of the table we use the same properties for fluids and tubes, but the extreme case of very short tubes ($R/L = 1$). In this case, the computed values of α are of order unity, thus reducing the value of the overall parameter $Nu/Gz^{1/3}$ in almost 17%, indicating that the Bird's solution, given by Eq. (39), is no longer valid, but instead Eq. (35) gives a better prediction.

The conjugated heat transfer process of a power-law fluid with a fully developed velocity profile in contact with the internal surface of a heat conducting circular tube has been analyzed for large values of the suitable Graetz number, using asymptotic as well as numerical techniques. Due to the finite thermal conductivity of the wall material and the imposed heat transfer on the external surface of the tube, the heat transfer by conduction along the wall is a relevant mechanism that can substantially modify the previous estimations of the local and global Nusselt numbers based in prescribed boundary conditions. The above is particularly valid for finite values of the parameter α/ε^2. In this sense, the local heat forced laminar convection through the inner surface of the circular tube, controlled by the axial heat conduction in the tube wall, governs the spatial evolution of the wall temperature. However, these particular temperature profiles are limited by the assumed values of the power index n of the non-Newtonian fluid.

References

[1] G.M. Elphingstone Jr., K.L. Greenhill, J.J.C. Hsu, Modeling of multiphase wax deposition, ASME J. Energy Resour. Technol. 121 (1999) 81–85.

[2] F.S. Ribeiro, P.R. Souza Mendes, S.L. Braga, Obstruction of pipelines due to paraffin deposition during the flow of crude oils, Int. J. Heat Mass Transfer 40 (1997) 4319–4328.

[3] R.P. Chhabra, J.F. Richardson, Non-Newtonian Flow in the Process Industries: Fundamentals and Engineering Applications, Butterworth-Heinemann, Great Britain, 1999.

[4] Y.I. Cho, J.P. Hartnett, Non-Newtonian fluids in circular pipe flow, Adv. Heat Transfer 15 (1982) 59–141.

[5] J.P. Hartnett, Y.I. Cho, Handbook of Heat Transfer, third ed., McGraw-Hill, New York, 1998.

[6] A. Lawal, A.S. Mujumdar, Laminar duct flow and heat transfer to purely viscous non-Newtonian fluids, in: A.S. Mujumdar, R.A. Mashelkar (Eds.), Advances in Transport Processes, Wiley, New York, 1989, pp. 352–443.

[7] A.H.P. Skelland, Non-Newtonian Flow and Heat Transfer, Wiley, New York, 1967.

[8] R.P. Chhabra, Heat and mass transfer in rheologically complex systems, in: D.A. Siginer, D. De Kee, R.P. Chhabra (Eds.), Advances in the Flow and Rheology of Non-Newtonian Fluids, Part B, Elsevier, New York, 1999, pp. 1435–1488.

[9] R.L. Pigford, Nonisothermal flow and heat transfer inside vertical tubes, Chem. Eng. Prog., Symp. Ser. 51 (1955) 79.

[10] R.B. Bird, Aur theorie des wärmeübergangs an nicht-Newtonsche flüssigkeiten bei laminarer rohrströmung, Chem. Ing. Tech. 31 (1959) 569.

[11] R.B. Bird, W.E. Stewart, E.N. Lightfoot, Transport Phenomena, Wiley, New York, 1960.

[12] M.A. Leveque, Les lois de la transmission de la chaleur par convection, Ann. Mines Mem. 13 (1928) 201–299.

[13] R.B. Bird, Viscous heat effects in extrusion of molten plastics, Soc. Plastics Eng. J. 11 (1955) 35–40.

[14] A.B. Metzner, R.D. Vaughn, G.L. Houghton, Heat transfer to non-Newtonian fluids, AIChE J. 3 (1957) 92–100.

[15] R. Mahalingam, L.O. Tilton, J.M. Coulson, Heat transfer in laminar flow of non-Newtonian fluids, Chem. Eng. Sci. 30 (1975) 921–929.

[16] S.M. Richardson, Extended Leveque solutions for flows of power-law fluid in pipes and channels, Int. J. Heat Mass Transfer 22 (1979) 1417–1423.

[17] T. Basu, D.N. Roy, Laminar heat transfer in a tube with viscous dissipation, Int. J. Heat Mass Transfer 28 (1985) 699–701.

[18] C.T. Liou, F.S. Wang, Solutions to the extended Graetz problem for a power-law fluid with viscous dissipation and different entrance boundary conditions, Numer. Heat Transfer A 17 (1990) 91–108.

[19] A. Lawal, A.S. Mujumdar, The effect of viscous dissipation in heat transfer to power-law fluids in arbitrary cross-sectional ducts, Warme-Stoffübertrag. 27 (1992) 437–446.

[20] A. Barletta, Fully developed laminar forced convection in circular ducts for power-law fluids with viscous dissipation, Int. J. Heat Mass Transfer 40 (1997) 15–26.

[21] P.R. Johnston, A solution method for the Graetz problem for non-Newtonian fluids with Dirichlet and Newmann boundary conditions, Math. Comput. Model. 19 (1994) 1–19.

[22] S. Bilir, Numerical solution of Graetz problem with axial conduction, Numer. Heat Transfer A 21 (1992) 493–500.

[23] K. Khellaf, G. Lauriat, A new analytical solution for the heat transfer in the entrance region for ducts: hydrodynamically developed flows of power-law fluids with constant wall temperature, Int. J. Heat Mass Transfer 40 (1997) 3443–3447.

[24] F. Méndez, C. Treviño, The conjugate conduction–natural convection heat transfer along a thin vertical plate with

non-uniform internal heat generation, Int. J. Heat Mass Transfer 43 (2000) 2739–2748.
[25] O. Bautista, F. Méndez, C. Treviño, Graetz problem for the conjugated conduction–film condensation process, ASME J. Thermophys. Heat Transfer 14 (2000) 1–7.
[26] C. Treviño, A. Espinoza, F. Méndez, Steady-state analysis of the conjugate heat transfer between forced counterflowing streams, ASME J. Thermophys. Heat Transfer 10 (1996) 476–483.
[27] A. Bejan, Convection Heat Transfer, Wiley, New York, 1995, pp. 122–124.
[28] M.J. Lighthill, Contributions to the theory of heat transfer through a laminar boundary layer, Proc. Roy. Soc. A 202 (1950) 359.
[29] F. Méndez, C. Treviño, Film condensation generated by a forced cooling fluid, Eur. J. Mech. B/Fluids 15 (1996) 217–240.
[30] G.B. Arfken, Mathematical Methods for Physicists, Academic Press, New York, 1970, pp. 734–736.